JOURNAL OF Materials CHEMISTRY

Preparation of silver ion conducting amorphous materials in the system Ag_2S–SiS_2 by mechanical milling processes

Huifen Peng,[a]† Nobuya Machida[a,b] and Toshihiko Shigematsu[a,b]

[a]*Department of Chemistry, Konan University, 8-9-1 Okamoto, Higashinada-ku, Kobe 658-8501, Japan. E-mail: peng@center.konan-u.ac.jp; Fax: +81-78-435-2539*
[b]*High Technology Research Center, Konan University, 8-9-1 Okamoto, Higashinada-ku, Kobe 658-8501, Japan*

Received 8th October 2001, Accepted 19th December 2001
First published as an Advance Article on the web 26th February 2002

Silver ion conducting amorphous materials in the system Ag_2S–SiS_2 were synthesized over the composition range from 0 to 60 mol% Ag_2S by use of a high-energy ball-milling process. The electrical and electrochemical properties of the obtained samples were evaluated by using ac impedance spectra, dc polarization measurements, and cyclic voltammetry. These measurements suggested that the silver-ion conductivities of the samples increased with an increase in the Ag_2S content and that the activation energy for conduction decreased with an increase in the Ag_2S content. The $60Ag_2S{\cdot}40SiS_2$ (mol%) sample showed its highest ion conductivity, 6.9×10^{-2} S m^{-1}, at 298 K in the system Ag_2S–SiS_2. This sample also possessed a wide electrochemical window over 2.0 V *vs.* Ag/Ag^+.

Introduction

Superion conducting glasses, which show high ionic conductivity in the range of 10^0–10^{-2} S m^{-1} at room temperature, have been extensively investigated for their promising applications as solid-state electrochemical devices, such as all-solid-state batteries, electrochromic devices, and so on. Among these glasses, silver ion conducting glasses containing AgI are the most widely studied as a model of superion conducting glasses because of their high ionic conductivity and good stability to air.[1-3] However, such AgI containing glasses are electrochemically decomposed at voltages higher than 680 mV (*vs.* Ag/Ag^+). This low decomposition voltage of the AgI-containing glasses limits their practical applications as solid electrolytes. This drawback is caused by the halide component of such glasses. Thus, halide-free silver ion conducting glasses are expected to have good electrochemical stability and a wide electrochemical window.

For lithium ion conducting glasses, similar problems are caused by lithium halide components. Glasses in the system LiI–Li_2S–P_2S_5 display high lithium ion conductivity of more than 10^{-1} S m^{-1} at room temperature. The decomposition voltages of these glasses, however, are lower than 2.0 V *vs.* Li/Li^+.[4] Consequently, the LiI containing glasses cannot be utilized as solid electrolytes for lithium batteries.

Kennedy *et al.*[5] reported that halide-free glasses in the Li_2S–SiS_2 system showed high lithium ion conductivities of over 10^{-2} S m^{-1} at room temperature and that the decomposition voltages of these glasses are larger than 8 V *vs.* Li/Li^+. These SiS_2 based glasses are reported to have higher lithium ion conductivities than other halide-free glasses based on glass-forming sulfides and oxides, such as B_2S_3, GeS_2, P_2S_5, B_2O_3, SiO_2, GeO_2, P_2O_5, *etc.*[6,7] From these observations, we expect glasses in the system Ag_2S–SiS_2 to have higher silver ion conductivity and good electrochemical stability.

Pradel *et al.*[8] reported that xAg_2S–$(100 - x)SiS_2$ glasses can be obtained over a very narrow composition range $50 \geqslant x \geqslant 40$ (mol%) by the twin-roller rapid quenching method. However, they did not report their electrochemical properties. The very narrow glass-forming region of the Ag_2S–SiS_2 glasses probably relates to the unstability of their melts at high temperature.

The high-energy ball-milling process is one of the most powerful methods for obtaining amorphous materials, intermetallic compounds, and metastable phases.[9–11] The high-energy ball-milling process is interesting as a new process for obtaining thermally unstable compounds at high temperature, because the process works at room temperature. In addition, the ball-milling process produces samples as fine powders. This point is also advantageous for obtaining ionic conductors, because solid electrolytes are usually used as powders in the fabrication of electrochemical devices such as solid-state batteries, capacitors, sensors, *etc.* Recently, Morimoto *et al.*[12,13] reported that amorphous substances were obtained in the system Li_2S–SiS_2 by the high-energy ball-milling process and they showed high lithium ion conductivities of more than 10^{-2} S m^{-1} at room temperature.

In the present study, we have applied the high-energy ball-milling process to the preparation of amorphous materials in the system Ag_2S–SiS_2, and have investigated the silver ion conducting properties of the obtained amorphous materials.

Experimental

Preparation of samples

Reagent-grade Ag_2S (Wako, 99%) and SiS_2 (Furuuchi, 99.9%) were used as raw materials. The desired amount of the raw materials was weighed and mixed in an agate mortar about 5 minutes beforehand. The mixture was placed in a stainless steel container with tetragonal zirconia balls (10 balls of 10 mm diameter and 30 balls of 5 mm diameter) and then the container was sealed with an O-ring. The total mass of the raw materials was 5 g. All the manipulations were carried out in a glove box filled with dry argon gas and thus milling was performed in an argon atmosphere. High-energy ball-milling was conducted using a planetary ball-milling apparatus (Fritsch, P-7) and the ball-milling rotation rate was 350 rpm.

The samples obtained were characterized by using X-ray

†*Permanent address*: Institute of Material Science & Engineering, Hebei University of Technology, Tianjin 300130, P. R. China.

 DOI: 10.1039/b109138g

diffraction measurements. For the measurements, the samples were sealed in an airtight container with beryllium windows and the container was mounted on an X-ray diffractometer (Rigaku, RINT2000) with Cu-Kα radiation.

Electrical measurements

The ball-milled sample was pressed into a pellet of 6 mm diameter and both sides of the pellet were coated with carbon paste to construct the electrodes. The total electrical conductivity of the pellet was measured in a dry argon atmosphere from 20 Hz to 1 MHz over the temperature range of 200 to 350 K with a precision LCR meter (Hewlett-Packard, HP4284A). The conductivity was determined by employing complex impedance analysis.

Wagner's dc polarization measurements were carried out at 273 K in a dry argon atmosphere to determine the electronic conductivities of the ball-milled samples. The mixture of metallic silver and the sample powders (1 : 1 in volume) was used as a reversible electrode for silver ions and graphite was used as a blocking electrode. A cell for this measurement was assembled as follows: the ball-milled sample was pressed into a pellet of 10 mm diameter and of 2 mm thickness, and then the mixture of silver and the sample powders was pressed on one side of the pellet. Subsequently, the graphite powder was pressed on the opposite side of the pellet. The cell was polarized by applying a constant dc potential over the range of 0.1 to 0.4 V across the blocking electrode (positive) and the reversible electrode (negative).

Cyclic voltammetry was also performed to estimate the electrochemical stability of the ball-milled samples at room temperature. The mixture of silver and the samples was used as counter and reference electrodes and the working electrode was nickel. The cyclic voltammogram was obtained over the potential range of -0.1 to 2.5 V at a scanning rate of 0.1 mV s^{-1} with a potentiostat (Hokuto, HA-501) and a function generator (Hokuto, HB-104).

Results and discussion

Fig. 1 shows the X-ray diffraction (XRD) patterns of ball-milled $60Ag_2S{\cdot}40SiS_2$ (mol%) samples. The XRD patterns of the raw materials, Ag_2S and SiS_2, are also shown in Fig. 1 for comparison. The milling time is denoted by MM and the XRD peaks with open circles and closed circles can be assigned to characteristic peaks of the raw materials Ag_2S and SiS_2, respectively. In the spectra of the samples ball-milled more than 6 h, the diffraction peaks of SiS_2 have disappeared and the peaks of Ag_2S become broader and the intensities of these peaks decrease with increasing milling time. The samples ball-milled more than 40 h show halo patterns in their XRD spectra, which indicates that the samples ball-milled for longer than 40 h become amorphous.

Fig. 2 shows the XRD spectra of the ball-milled samples with different Ag_2S contents. The spectrum of the ball-milled sample of pure SiS_2 is also shown in Fig. 2 for comparison. The milling time is also denoted by MM. These results indicate that the amorphous samples can be obtained over the wide composition range of 0 to 60 mol% Ag_2S by the high-energy ball-milling process. The color of the amorphous samples changes with their Ag_2S contents. The samples with 0 to 20 mol% Ag_2S are grey, those with 30 to 50 mol% Ag_2S are yellow and the 60 mol% Ag_2S containing sample is reddish brown.

The XRD spectra of the samples with low Ag_2S contents over the range of 0 to 20 mol% show two very broad peaks at around 14° and at around 30°. In contrast, the XRD spectra of the samples with an Ag_2S content of more than 30 mol% show only one broad peak at around 30°. This difference in the XRD spectra relates to the local structure around Si in these ball-milled samples. Crystalline SiS_2 has been reported to be

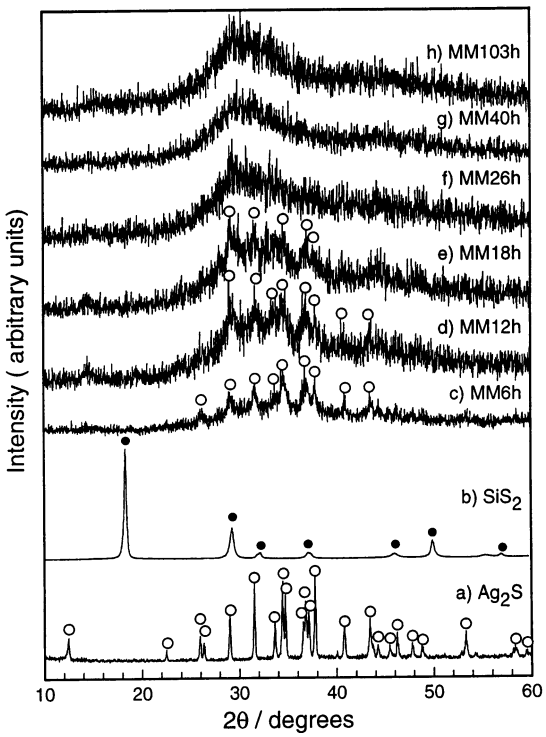

Fig. 1 XRD patterns of the ball-milled $60Ag_2S{\cdot}40SiS_2$ (mol%) sample, ○ Ag_2S and ● SiS_2 crystals.

constructed from

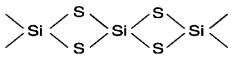

double chains, in which SiS_4 tetrahedra are connected each other by edge sharing.[14,15] These double chains are stacked by van der Waals forces in the SiS_2 crystal.[14,15] The ball-milled SiS_2 amorphous sample is probably constructed from the same SiS_2 chains, but the chains are stacked randomly. The mechanical force of the ball milling cleaves the van der Waals gaps and destroys the stacking structure.

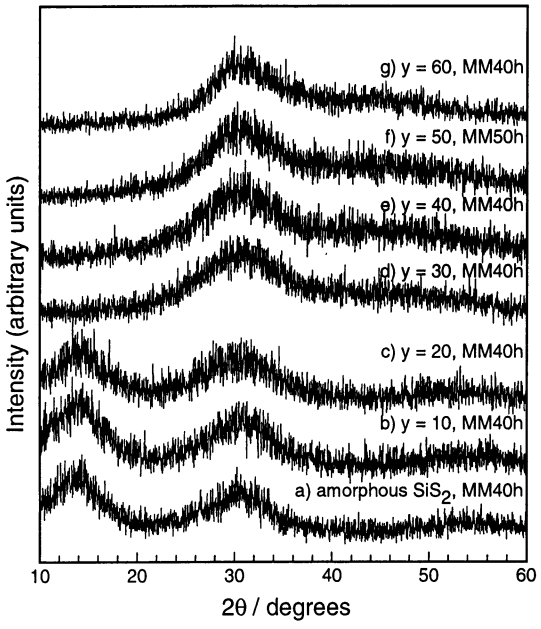

Fig. 2 XRD spectra of the ball-milled samples with different Ag_2S contents in the system $yAg_2S{\cdot}(100 - y)SiS_2$ (y = 0, 10, 20, 30, 40, 50, 60 mol%).

In contrast, another mechano-chemical reaction could also occur in the Ag_2S containing samples during the ball-milling process. The Ag_2S could react with a bridging sulfur of SiS_2 to form a non-bridging sulfur according to eqn. (1).

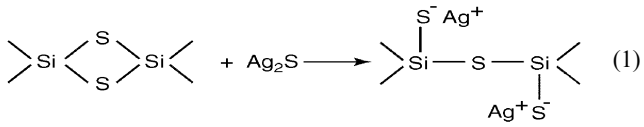

(1)

Through the reaction, the double-chain structure of SiS_2 changes into a single-strand structure, and the edge-sharing connection between the SiS_4 tetrahedra changes into a corner-sharing connection between the tetrahedra. If all of the Ag_2S added to the sample reacts with SiS_2 according to eqn. (1), a simple calculation predicts that 33 mol% Ag_2S is sufficient to make all the double-chain structure change into the single-chain structure. Such structural changes of the ball-milled samples probably relates to the difference in the XRD patterns between the samples with an Ag_2S content of lower than 20 mol% and the samples with an Ag_2S content higher than 30 mol%. We are currently trying to confirm these structural changes in the ball-milled samples by means of ^{29}Si MAS-NMR and Raman scattering measurements. We will deal with the structural study as a separate paper in the near future.

Fig. 3 shows the amorphous-sample-forming region in the system Ag_2S–SiS_2 obtained by the high-energy ball-milling process. The abscissa of Fig. 3 indicates the Ag_2S content and the ordinate is the milling time. In Fig. 3, open circles, open triangles and closed triangles denote amorphous, partially crystalline, and crystalline samples, respectively. The main crystalline phase in the open triangle and closed triangle samples is the Ag_2S crystalline phase. The region of amorphous-sample formation is much wider than the glass-forming region reported for the melt quenching methods of Pradel *et al.*[8]

As an example of the ac conductivity measurements, the complex impedance plots for a 40 h-ball-milled $40Ag_2S{\cdot}60SiS_2$ sample at various temperatures are shown in Fig. 4. The bulk impedance is attributed to the semicircle in the high frequency range and the straight line in the low frequency range observed

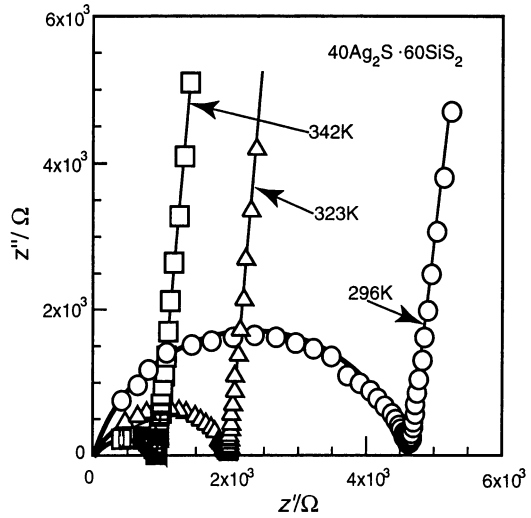

Fig. 4 Complex impedance plots of the 40 h-ball-milled $40Ag_2S{\cdot}60SiS_2$ sample at various temperatures.

at each temperature. The bulk resistance is identified as the intersecting point of the semicircle with the real axis.

Fig. 5 shows the temperature dependence of the conductivity for the ball-milled samples with different Ag_2S contents. The conductivities, σ, fit the Arrhenius equation [eqn. (2)]

$$\sigma T = A\exp(-E_a/RT) \quad (2)$$

where T is the absolute temperature, A the pre-exponential, E_a the activation energy for conduction, and R the gas constant.

The conductivities at 298 K, σ_{298}, and the activation energy for conduction, E_a, are shown in Figs. 6(a) and 6(b), respectively, as a function of composition. The value of σ_{298} tends to increase with an increase in the Ag_2S content. This tendency is reasonable because the number of charge carriers increases with an increase in the Ag_2S content. It is noteworthy, however, that the conductivity begins to level off at a composition of about 50 mol% Ag_2S. This levelling-off tendency is probably caused by the increasing number of

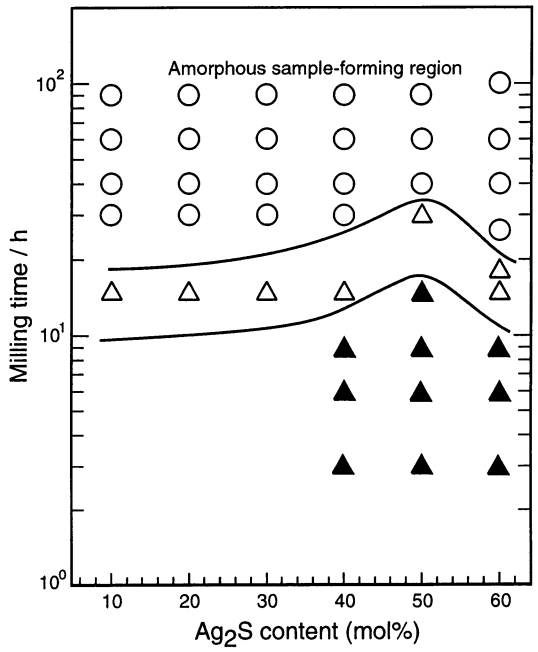

Fig. 3 The region amorphous-sample formation in the system Ag_2S–SiS_2 obtained by the high-energy ball-milling process; ○: amorphous, Δ: partially crystalline, and ▲: crystalline samples.

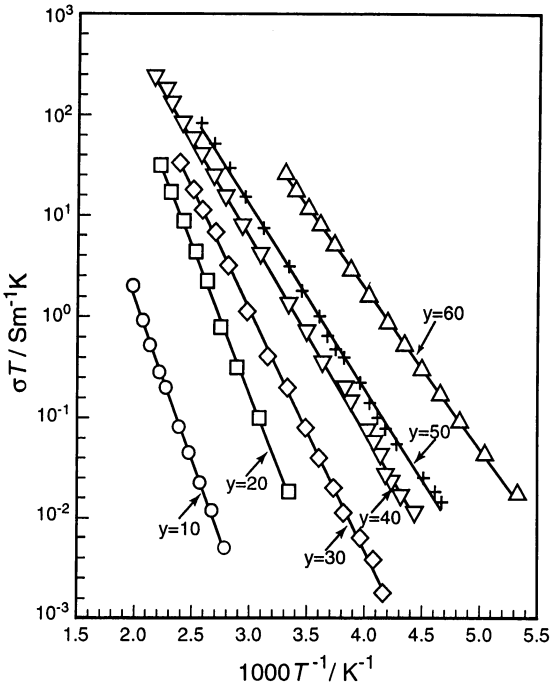

Fig. 5 Temperature dependence of the conductivities for the ball-milled samples with different Ag_2S contents.

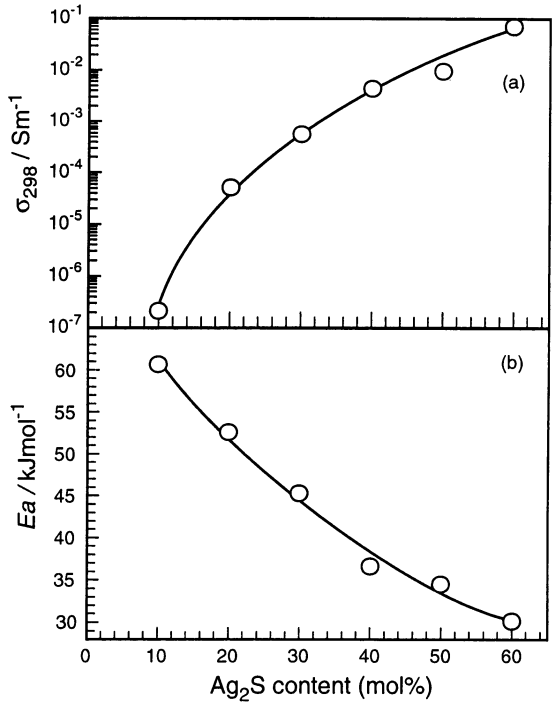

Fig. 6 The electrical conductivities at 298 K, σ_{298}, and the activation energies for conduction, E_a, of the ball-milled samples as a function of Ag_2S content.

non-bridging sulfurs, which act as trapping sites of mobile silver ions. The activation energy, E_a, of the samples obtained decreases with an increase in the Ag_2S content, which explains the tendency towards increasing conductivities described above.

Fig. 7 shows the current–voltage characteristics for the determination of electronic conductivities by use of a cell (−) Ag|sample|C (+). According to the Wagner polarization analysis,[16] the total electronic current, I, is given by eqn. (3), where I_e and I_h are the currents due to electrons and holes, respectively, R is the gas constant, T is the absolute temperature, A is the electrode area, L is the sample thickness, F is the Faraday constant, E is the applied voltage, and σ_e and σ_h are the conductivities due to electrons and holes, respectively.

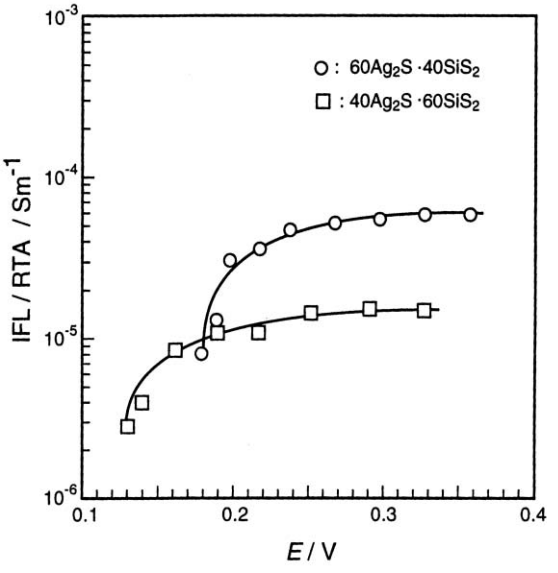

Fig. 7 Current *vs.* voltage characteristics of the ball-milled $40Ag_2S{\cdot}60SiS_2$ (mol%) and $60Ag_2S{\cdot}40SiS_2$ (mol%) samples at 273 K for the determination of electronic conductivities.

Table 1 Ion and electronic conductivities at 273 K and ion transport number of the ball-milled samples, $40Ag_2S{\cdot}60SiS_2$ and $60Ag_2S{\cdot}40SiS_2$ (mol%)

Composition (mol%)	σ_{273}/S m^{-1}	σ_e/S m^{-1}	t_i
$40Ag_2S{\cdot}60SiS_2$	1.46×10^{-3}	1.4×10^{-5}	0.990
$60Ag_2S{\cdot}40SiS_2$	2.49×10^{-2}	6.0×10^{-5}	0.998

Usually the electron conductivity is due to either electrons and/or holes. If $\sigma_e \gg \sigma_h$, the term $\sigma_h[\exp(EF/RT) - 1]$ is negligible and I becomes independent of E. If $\sigma_e \ll \sigma_h$, the term $\sigma_e[1 - \exp(-EF/RT)]$ is negligible and I increases exponentially with E. The current–voltage characteristics shown in Fig. 7 indicate that the relation $\sigma_e \gg \sigma_h$ holds for these samples. The electronic conductivities σ_e at 273 K, determined from eqn. (3), are shown in Table 1, with the ac conductivities at 273 K, σ_{273}. The electronic conductivities are lower by 2 to 3 orders of magnitude than the total ac conductivities. The ion transport numbers, t_i, calculated from the total and electronic conductivities are also shown in Table 1. It is evident that the transport number of the silver ions is practically unity.

$$I = I_e + I_h = RTA/FL\{\sigma_e[1 - \exp(-EF/RT)] + \sigma_h[\exp(EF/RT) - 1]\} \quad (3)$$

Fig. 8 shows the cyclic voltammogram of the 40 h-ball-milled $60Ag_2S{\cdot}40SiS_2$ sample at a scanning rate 0.1 mV s^{-1}. The initial voltage of the test cell is 0.09 V *vs.* Ag/Ag$^+$. In the first step, the potential of the cell is cathodically swept to −0.1 V. A cathodic current peak is observed below 0 V during this sweep. The current corresponds to the deposition of metallic silver on the nickel working electrode. After that, the direction of the voltage sweep is reversed and the voltage is anodically swept until 2.5 V *vs.* Ag/Ag$^+$. During the anodic sweep, an anodic current peak is observed at around 0.07 V, and the anodic peak is attributed to the dissolution of the silver metal that has deposited on the working electrode during the cathodic sweep. The coulombic efficiency, which is determined from the ratio of the area of the anodic peak to that of the cathodic peak, is 0.997. This result suggests that the ball-milled amorphous-$60Ag_2S{\cdot}40SiS_2$ sample has a superior reversibility of the deposition and dissolution of silver. Moreover, there is no current peak except the peaks corresponding to the deposition and dissolution of silver over the whole range from −0.1 to 2.5 V. This result suggests that the electrochemical window of the sample is wider than 2.5 V *vs.* Ag/Ag$^+$ at room temperature.

Hence, it can be concluded that the $60Ag_2S{\cdot}40SiS_2$ sample prepared by the ball-milling process has suitable electrochemical properties to act as solid electrolytes for all-solid-state batteries.

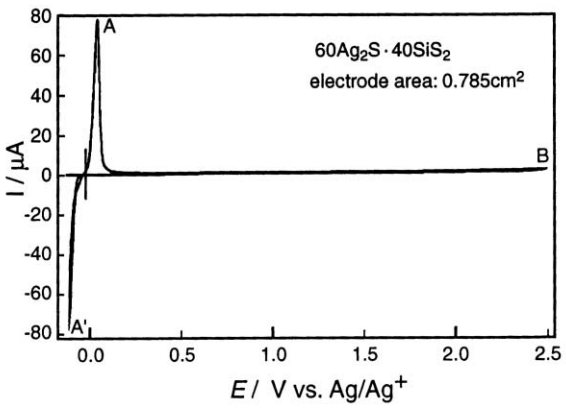

Fig. 8 Cyclic voltammogram of the 40 h-ball-milled $60Ag_2S{\cdot}40SiS_2$ sample at a scanning rate 0.1 mV s^{-1}.

Conclusions

Silver ion conducting materials have been synthesized for the system Ag_2S–SiS_2 by using the high-energy ball-milling process. Ball milling of more than 30 h gave the samples in an amorphous state over the wide composition range 0 to 60 mol% Ag_2S. The silver ion conductivities of the amorphous samples obtained increased with an increase in the Ag_2S content, and the activation energy for ion conduction correspondingly decreased with an increase in the Ag_2S content. The amorphous sample obtained with a 60 mol% Ag_2S content showed the highest silver ion conductivity 6.9×10^{-2} S m^{-1} at room temperature. Electronic conductivity of the sample was estimated to be 6.0×10^{-5} S m^{-1} by Wagner's polarization methods and hence the ion transport number of the sample was almost unity. Cyclic voltammetry showed that the amorphous-$60Ag_2S{\cdot}40SiS_2$ (mol%) sample had a wide electrochemical window of more than 2.5 V *vs.* Ag/Ag^+.

Acknowledgement

The authors wish to thank Mr Masahiko Kikuchi for his technical assistance. This research was supported by a Grant-in Aid for Scientific Research from the Ministry of Education, Science, Sports and Culture of Japan.

References

1 T. Minami, K. Imazawa and M. Tanaka, *J. Non-Cryst. Solids*, 1980, **42**, 469.
2 T. Minami, in *Materials for Solid State Batteries*, ed. B. V. R. Chowdari and S. Radhakrishna, World Scientific, 1986, p. 169.
3 A. Schiraldi and E. Pezzati, *Mater. Chem. Phys.*, 1989, **23**, 75.
4 R. Mercier, J. P. Malugani, B. Fahys and G. Robert, *Solid State Ionics*, 1981, **5**, 663.
5 J. H. Kennedy, Z. Zhang and H. Eckert, *J. Non-Cryst. Solids*, 1990, **123**, 328.
6 A. Pradel and M. Ribes, *Mater. Chem. Phys.*, 1989, **23**, 121.
7 J. H. Kennedy, *Mater. Chem. Phys.*, 1989, **23**, 29.
8 A. Pradel, G. Taillades, M. Ribes and H. Eckert, *J. Non-Cryst. Solids*, 1995, **188**, 75.
9 C. Koch, O. B. Cabin, C. G. Mckamey and J. O. Scabrough, *Appl. Phys. Lett.*, 1983, **43**, 1017.
10 T. Fukunaga, S. Kajikawa, Y. Hokari and U. Mizutani, *J. Non-Cryst. Solids*, 1998, **232–234**, 465.
11 J. Wang, X. Junmin, W. Dongmei and N. Weibeng, *Solid State Ionics*, 1999, **124**, 271.
12 H. Morimoto, H. Yamashita, M. Tatsumisago and T. Minami, *J. Am. Ceram. Soc.*, 1999, **82**, 1352.
13 H. Morimoto, H. Yamashita, M. Tatsumisago and T. Minami, *J. Ceram. Soc. Jpn.*, 2000, **108**, 128.
14 A. F. Wells, in *Structural Inorganic Chemistry*, 5th edn., Oxford Science Publications, 1984, p. 983.
15 M. Tenhover, M. A. Hazel and R. K. Grasseli, *Phys. Rev. Lett.*, 1983, **51**, 404.
16 C. Wagner, in *Proc. C. I. T. C. E., Electrochem. Semicond.*, 1955, p. 361.